

Triple Band Compact Textile Antenna Structure for Wearable Applications

Shankar Bhattacharjee^{1,*} and Monojit Mitra²

¹Department of Electronics & Communication Engineering, Indian Institute of Information Technology, Nagpur, India

²Department of Electronics & Telecommunication Engineering
Indian Institute of Engineering Science & Technology, Shibpur, India

ABSTRACT: A compact triple band antenna for wearable applications is presented in this paper. The antenna exhibits dual mode operation for ON/OFF body communication. The antenna has a patch like radiation pattern for OFF body communication and quasi-monopole like radiation pattern for ON body communication. Triple bands are achieved by incorporating an annular ring patch with the triangular patch. Tuning of the antenna and impedance matching has been done using two open ended rectangular slots and two shorting pins. As a result, the antenna has a patch like radiation pattern at frequencies 2.5 GHz (ISM band), 3.5 GHz (Wi Max band), and quasi-monopole like radiation pattern at 5.5 GHz (WLAN band). The proposed antenna is compact in nature with a size of $70 \times 70 \times 2.1 \text{ mm}^3$. User comfort has been taken into care with the use of all textile materials to fabricate the antenna except the SMA connector. A full ground plane in the proposed antenna ensures minimum coupling with human body and thereby a low SAR (specific absorption rate) value. Investigation of the antenna has been performed in both free space and on body scenarios.

1. INTRODUCTION

The field of wearable devices has witnessed tremendous advancements in recent times. Wearable devices have a wide range of applications ranging from real time tracking, monitoring, entertainment, military applications, healthcare, etc. Antenna is one of the crucial front-end parts of the wearable device. The research on body wearable antennas evolved rapidly in recent times. The wearable devices collect information about temperature, pressure, blood glucose levels, pH from other body worn devices and transmit it to nearby base stations respectively. In such scenarios, a multi-band antenna with a certain radiation pattern at each band is required.

Recent research work in the domain of wearable antennas pertains to multiband operations, which are easy to fabricate, provide high gain, and have a very low specific absorption rate (SAR), so that they both cater to comfort and fulfil the plethora of standards set for practical usage. The objective for present-day designers is to provide a multi-purpose antenna, with good acceptable gain, large bandwidth, and small size.

Many tri-band antennas have already been reported in literature by using different techniques such as: three different plates, which were shorted to ground [1], U-slots on the rectangular patch [2–4], planar inverted-F patch antenna [5], proximity fed stacked patch antenna [6], a microstrip slot with an etched ground plane [7], and a substrate integrated waveguide (SIW) based wearable equilateral triangular leather antenna [8]. However, present ongoing trends on wearable antennas include dual modes, i.e., on-body and off-body modes of operation, in

multiple bands. These antennas are expected to provide different radiation characteristics at each band, for example plane polarization and perpendicular polarization to human body for off- and on-body links, respectively. In this case, a single antenna would serve the purpose of two antennas. Numerous antennas have been proposed recently: a dual-band dual-mode circular textile antenna with two slots and a shorting pin [9] and a half-circular patch with a half-ring, loaded with two shorting pins and a slot on the ground plane [10]. A dual-mode triple-band helix antenna has been suggested for satellite navigation system [11]. For wearable body centric communication, we need to have both patch type and vertical monopole type radiation patterns, to communicate with devices outside the body and on body, respectively.

In this paper, a triple-band antenna with different radiation patterns for body centric communication is presented. The proposed antenna supports OFF body communications at 2.5 GHz and 3.5 GHz, and in addition to that it also supports ON body communication at 5.5 GHz WiMAX band. With the advancements of wireless body area networks, there are more functional requirements of wearable devices. For supporting multiple functionalities at the same time, multi-band operation is required. Unlike the previously mentioned designs, made of rigid materials, this antenna is made of flexible textile material felt. The antenna is compact in nature, and a full ground plane is maintained on the opposite side of the patch antenna, which provides a high degree of isolation from the human body, and consequently a low SAR value is achieved.

* Corresponding author: Shankar Bhattacharjee (shankarsam68@gmail.com).

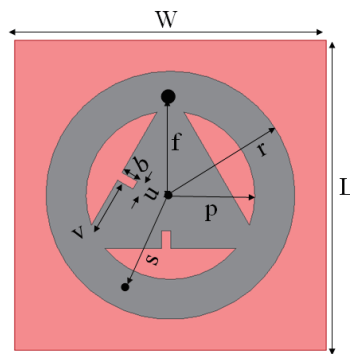


FIGURE 1. Geometry of the proposed antenna.

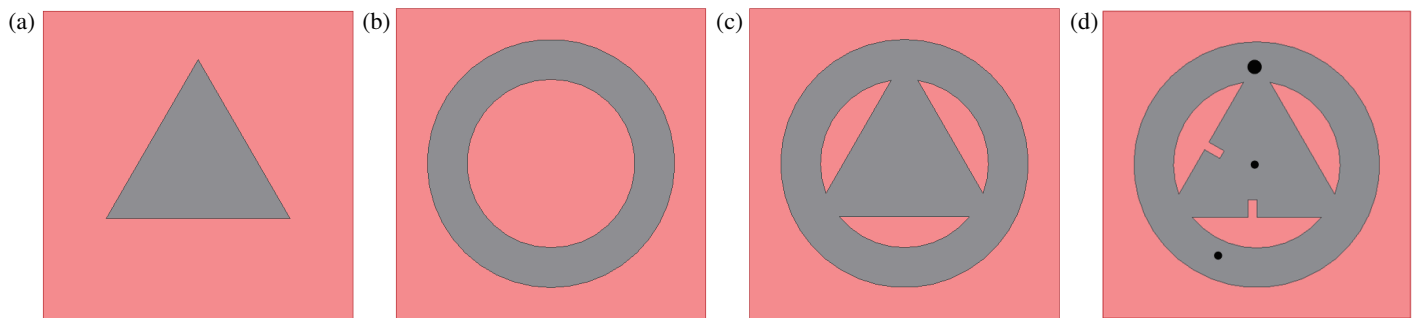


FIGURE 2. Evaluation steps of the antenna. (a) Triangular Patch (Model 1). (b) Annular ring patch (Model 2). (c) Composite antenna (Model 3). (d) Composite antenna with reactive loadings (Proposed Antenna).

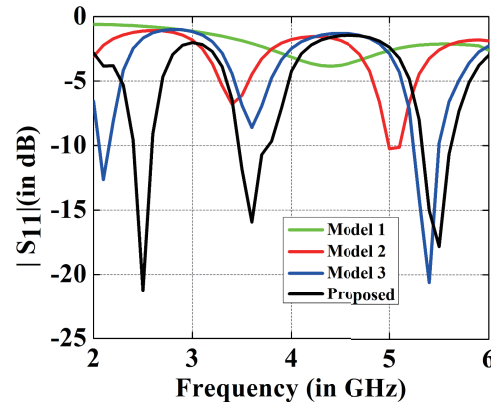


FIGURE 3. Simulated S_{11} values for different models.

2. ANTENNA DESIGN

The proposed antenna, as shown in Fig. 1, is a new approach to get the triple band. A coaxial feed is given, which is easy to fabricate, gives a good impedance matching, and suppresses the spurious radiation. The annular ring is chosen with an outer radius and inner radius of 28 and 19 mm, respectively. It is integrated with an equilateral triangle patch of height 36 mm.

The felt material used as substrate has a relative permittivity of 1.634 and a thickness of 2.1 mm. The measurement has been performed by using Agilent dielectric measurement probe kit. Woven conductive silver fabric material has been used for the realization of the patch and ground plane. Fabric based stainless steel thread, of 0.11 mm radius, is used as shorting pins near the

center of the triangle and on the annular ring designated as (S_1 and S_2). Soldering is performed using conductive silver paste. The dimensions of different sections of the antenna in mm are $W = L = 70$, $r = 28$, $p = 19$, $f = 23$, $b = 2$, $u = 1$, $s = 20$, $v = 12$, respectively.

The evolution of the triple-band antenna is depicted in Figs. 2(a)–(d). An annular ring is integrated with an equilateral triangular patch having two open ended slots on the triangle and two shorting pins to have the desired resonating frequencies. The objective is to achieve the patch type radiation pattern at both f_1 and f_2 for off-body and vertical monopole type in f_3 for on-body, thus fulfilling the requirement of body centric communication. The S_{11} values for different models of the

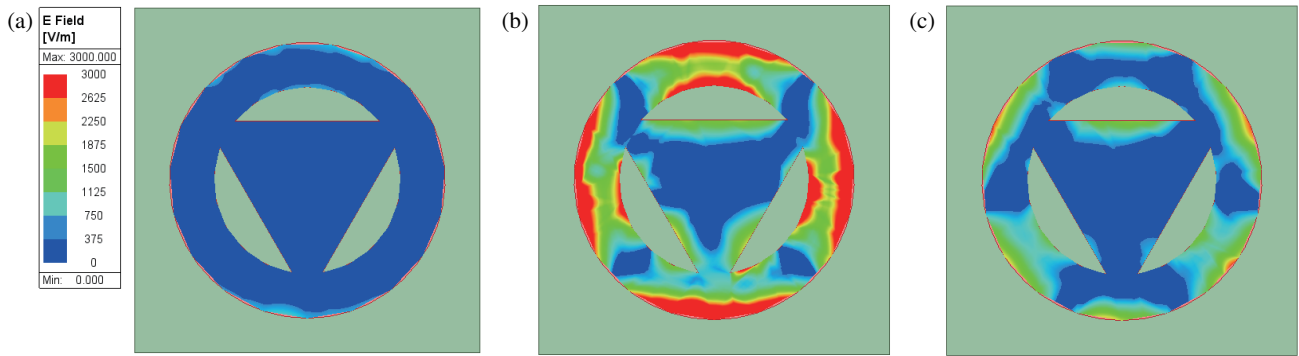


FIGURE 4. *E*-Field distribution before placing shorting pins at (a) 2.5 GHz (b) 3.5 GHz and (c) 5.5 GHz.

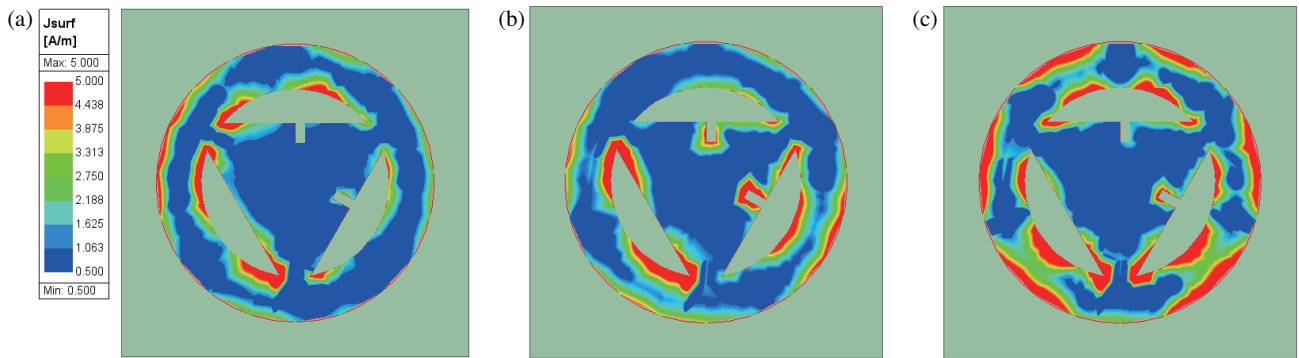


FIGURE 5. Current distribution with reactive loadings at (a) 2.5 GHz (b) 3.5 GHz and (c) 5.5 GHz.

antenna are shown in Fig. 3. Model 1 has quite low S_{11} value, and model 2 of the antenna radiates at two different frequencies within the range of interest. Incorporating the triangular patch with the annular patch results in triple band operation but not at the designated frequencies. With the application of slot and shorting pin loading, the frequency ratio is controllable where the proposed antenna is now radiating at 2.5, 3.5, and 5.5 GHz, respectively.

3. ANALYSIS AND RESULTS

The resonant frequency f_{mn} of the triangular patch antenna can be calculated using a well-known formula:

$$f_{mn} = \frac{2c(m^2 + mn + n^2)^{1/2}}{3s_e \sqrt{\epsilon_e}} \quad (1)$$

where s_e is the effective side length; ϵ_e is the effective permittivity; c is the speed of light; m, n correspond to modes of the antenna.

For a fixed geometry patch, the ratio of resonance frequencies is fixed for a particular mode [12, 13]. Reactive loading technique, viz, introduction of slots and shorting pins is used to overcome the above-mentioned problem.

The electric field distribution of the proposed antenna without any type of reactive loading is shown in Figs. 4(a)–(c). The *E*-field distribution of the antenna gives insight to different mode generation of the annular ring and the triangular patch.

The triangular patch antenna initially without any type of reactive loadings resonates at around 4.5 GHz. With the addition of the annular ring around the triangular patch, the antenna starts radiating at 2.1, 3.7, and 5.4 GHz. To match the resonating frequencies of the composite antenna for the intended application bands, reactive loading technique has been employed with the use of shorting pins and rectangular slots. The electric field distribution of the proposed antenna without any type of reactive loading is shown in Figs. 5(a)–(c). The shorting pins were placed in the electric field null position at 3.5 GHz. At 2.5 GHz, maximum current magnitude is around an annular ring patch. The triangular patch antenna plays a major role at 3.5 GHz while both triangular and annular ring patches are responsible for the higher band, i.e., 5.5 GHz. The first two bands have a broadside radiation pattern while the third band has a quasi-monopole type radiation pattern.

3.1. Effect of Shorting Pins

In order to observe the effect of shorting pins and slot over the composite antenna, parametric analysis has been performed. When shorting pin 1 ‘ S_1 ’ is placed at positions symmetric to both x and y -axes in all four quadrants, it affects impedance matching, while resonant frequencies remain unchanged, as shown in Fig. 6(a). The second shorting pin ‘ S_2 ’ is placed on the annular ring patch, and the position is varied symmetrically as shown in Fig. 6(b). The position of the second shorting pin

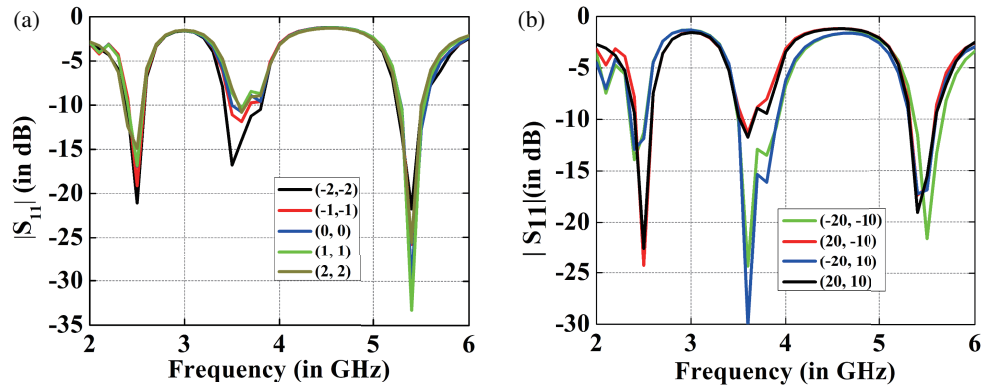


FIGURE 6. Parametric analysis for shorting pin position variation. (a) S_{11} variation for S_1 , (b) S_{11} variation for S_2 .

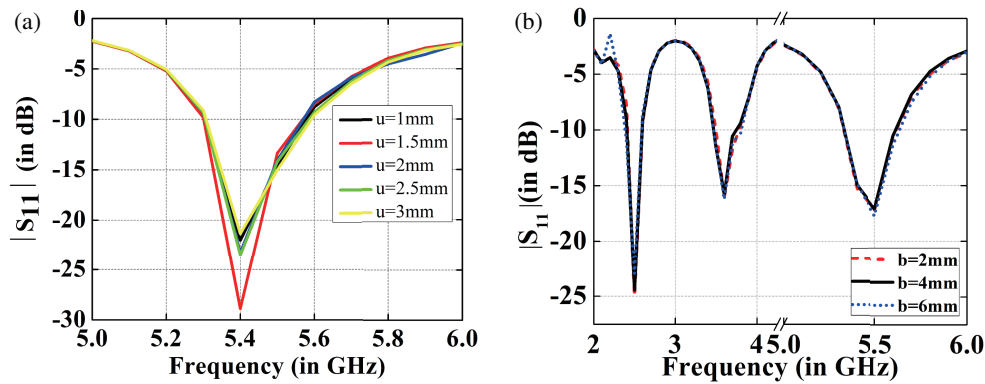


FIGURE 7. Simulation results of S_{11} variation with. (a) Width variation. (b) Length variation.

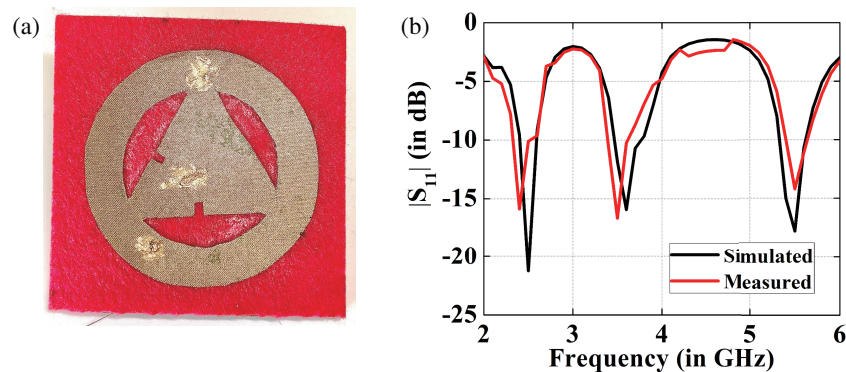


FIGURE 8. (a) Fabricated model. (b) Simulated and measured results.

mainly varies the impedance matching of 1st and 2nd bands, respectively.

3.2. Effect of Open-Ended Slots

Two open ended rectangular slots have been carved over the triangular patch. The variation of the width of the slot basically affects the return loss of the 3rd band as shown in Figs. 6(a) and (b).

Variation in length of the slot is not found to be effective over the performance of the antenna as shown in Fig. 7(b). The two

parameters, i.e., length and width of the slots, were optimized in such a way to achieve the best results.

4. ANTENNA PERFORMANCE

The experiment was carried out both in free space and on body environment for performance validation. The fabricated antenna is shown in Fig. 8(a). The measured and simulated $|S_{11}|$ characteristics are shown in Fig. 8(b) and are in good agreement. There is a slight shift in the frequencies in simulated and measured results, due to the tolerances of fabrication, in manual cutting of textile material and silver sheet. The sim-

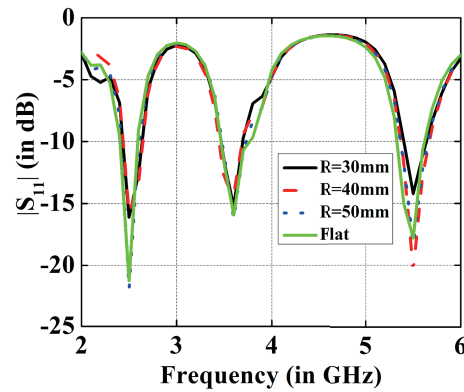


FIGURE 9. Simulated S_{11} values at different radii.

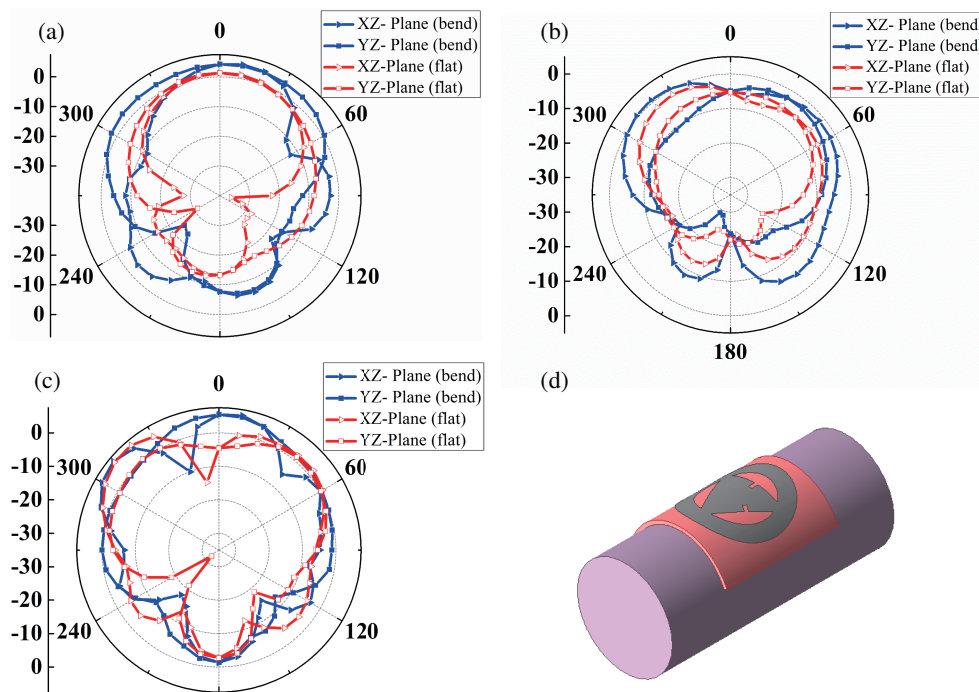


FIGURE 10. Results-Far-field radiation patterns under flat and bend conditions at (a) 2.5 GHz (b) 3.6 GHz (c) 5.5 GHz (d). Bend model of the antenna.

ulated -10 dB bandwidth is 190 MHz (2.40–2.59 GHz) in f_1 , 300 MHz (3.46–3.76 GHz) in f_2 , 300 MHz (5.32–5.62 GHz) in f_3 while measured one is 200 MHz (2.40–2.6 GHz) in f_1 , 285 MHz (3.46–3.74 GHz) in f_2 , 290 MHz (5.42–5.61 GHz).

The bending effect on antenna is also tested under different bending conditions to show its suitability under practical conditions. Bending is performed by wrapping antenna with cylinders of radii 30, 40, and 50 mm. Fig. 9 shows the simulated bending results at given radii. When bending is done on cylinder of radius 50 mm, there is literally no effect on bandwidth and resonant frequencies, but when it's done on cylinder of 30 mm, the frequencies f_1 and f_3 shift by 20 MHz to the right, and on 40 mm radius, f_1 shifts by 10 MHz, while there is no reduction in bandwidth for all conditions. The radiation patterns of the antenna under conformal and flat conditions are also shown in Figs. 10(a)–(c). The bending model is shown in Fig. 10(d).

The measured far-field radiation patterns of the proposed antenna, at the resonant frequencies 2.5, 3.5, and 5.5 GHz for both XZ and YZ planes are shown in Figs. 11(a)–(f).

At 2.5 GHz, the antenna has a patch like radiation which is applicable to off-body communication links. At 5.5 GHz, the patch radiates like a quasi-monopole antenna, which is applicable to on-body communication links.

Figure 12 shows the measured peak gain of the proposed antenna in free space and on phantom model. The peak gains of the antenna on phantom at 2.5, 3.5, and 5.5 GHz band are 2.2, 0.3, and 4.4 dBi, respectively.

Finally, adherence to Federal Communications Commission (FCC)'s guidelines on human exposure to radio-frequency (RF) fields, the SAR level of the proposed antenna was investigated with a three layer human phantom model comprising skin, fat, and muscle. The antenna is placed over $100 \text{ mm} \times 100 \text{ mm} \times$

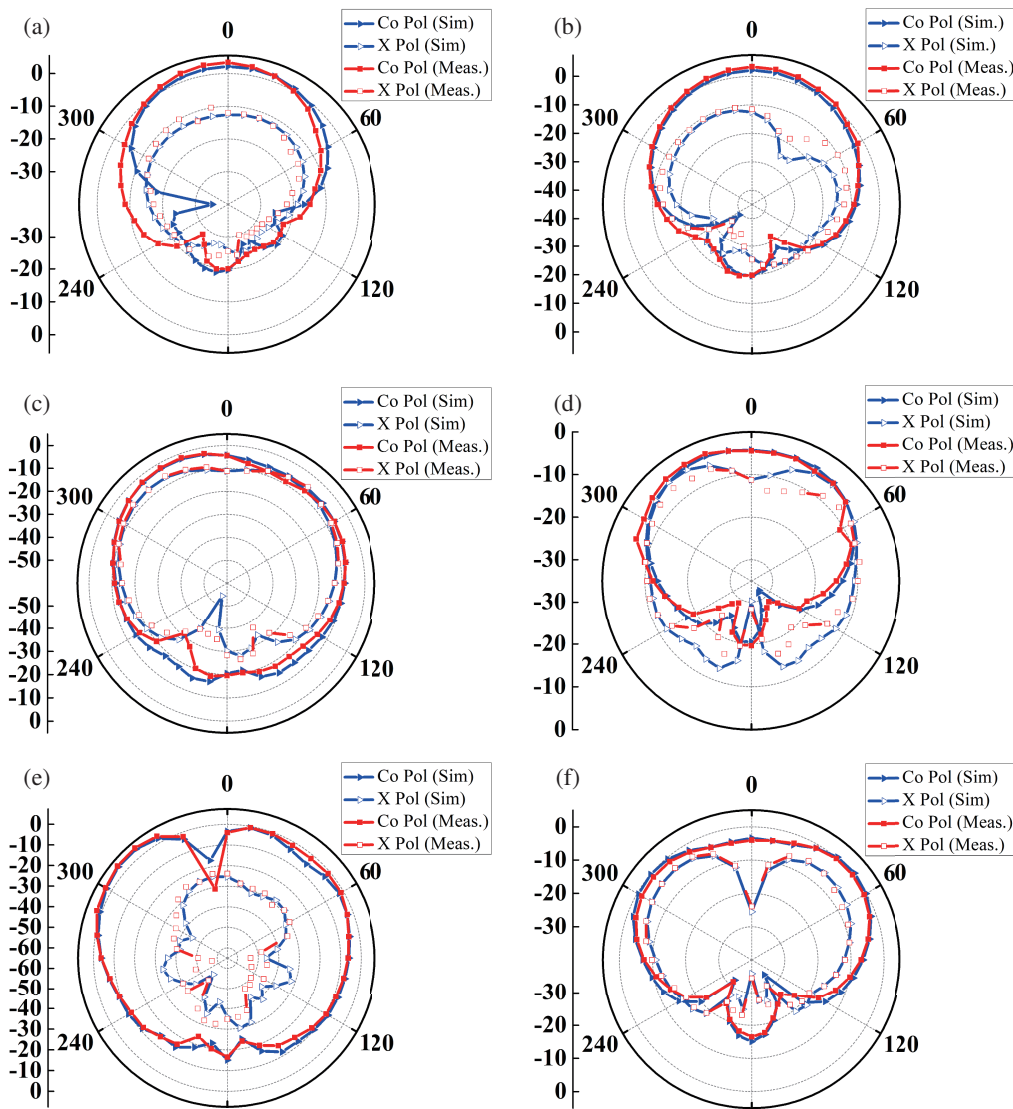


FIGURE 11. Results-Far-field radiation patterns for XZ and YZ Planes at (a), (b) 2.5 GHz (c), (d) 3.5 GHz (e), (f) 5.5 GHz.

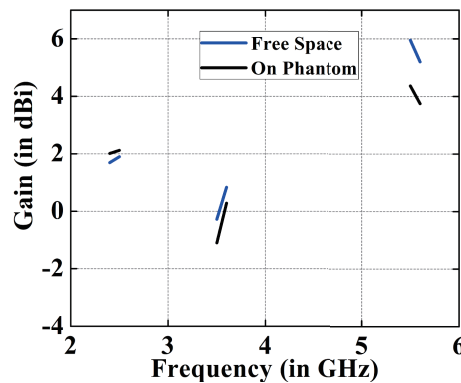


FIGURE 12. Gain variation with frequency.

50 mm human body phantom which has the electrical properties obtained from [16].

The three-layered phantom model and SAR simulation results are shown in Figs. 13(a)–(d). SAR levels have been investigated, based on the IEEE C95.1-1999 standard, averaged

over 1 gm of tissue with the input power of 750 mW. Maximum 1 gm averaged SAR at 2.5, 3.5, and 5.5 GHz are 0.31, 0.57, and 1.47 W/kg, respectively, which are below 1.6 W/kg [17].

A comparison is given in Table 1, which compares the proposed tri-band patch antenna with previously reported works.

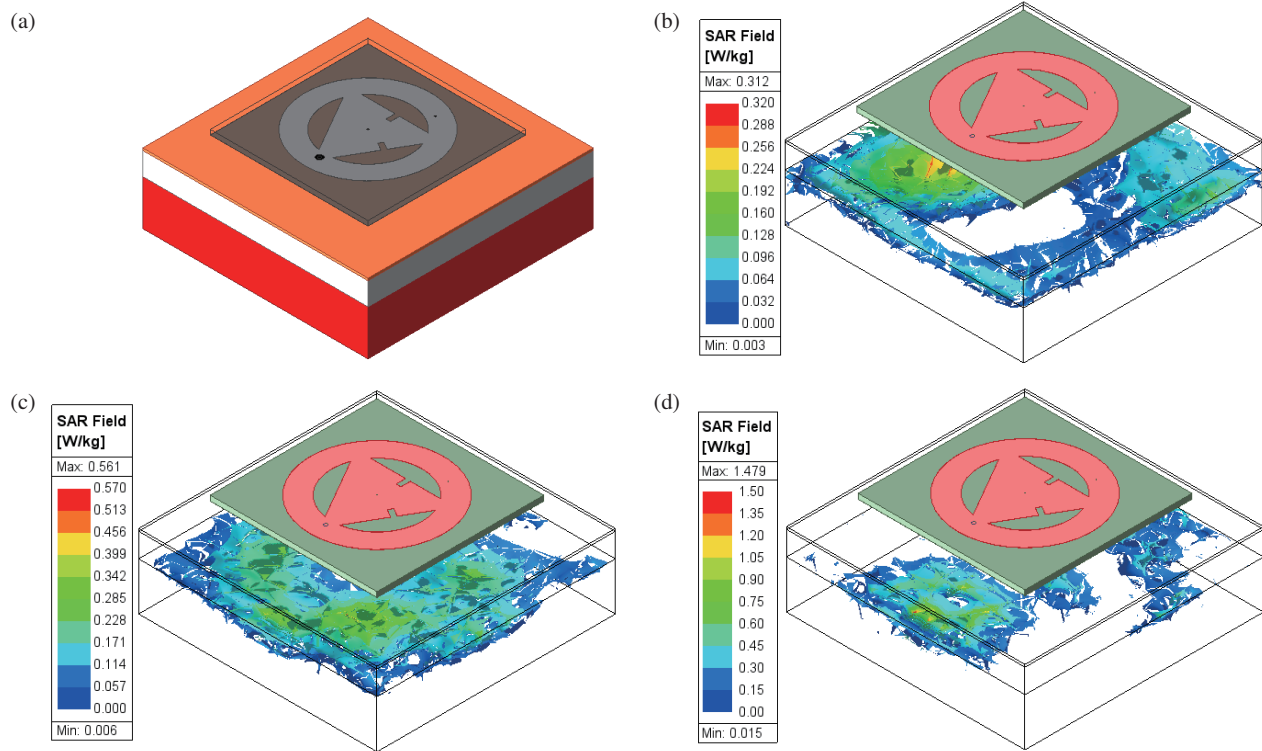


FIGURE 13. Three layer phantom model SAR value at (a) 2.5 GHz (b) 3.5 GHz (c) 5.5 GHz.

TABLE 1. Comparison table with other reported works.

Ref.	Substrate	Volume (in mm ³)	f_r (in GHz)	Bandwidth (in MHz)	Gain (in dBi)
[8]	Denim	140 × 60 × 0.78	0.915, 2.45, 5.8	130, 180, 1550	2.03, 2.45, 4.31
[14]	Jeans cotton	260 × 100 × 3	0.45, 0.8, 1.4	-	2.1, 2.7, 3.7
[15]	Leather	80 × 80 × 2	2.4, 3.51, 4.69	60, 58, 101	1.1, 0.9, 2.1
[18]	Rubber	80 × 75 × 1.64	0.9, 1.8	70, 175	7.46, 8.13
[19]	Rogers Duroid RO3003	41 × 41 × 1.52	2.4, 5.8	91.2, 301.6	4.84, 5.87
[20]	Taconic TLY-5 and felt	60 × 60 × 8.72	2.4, 3.45	141.1, 162.2	6.7, 8.9
[21]	Felt	100 × 100 × 2	2.4, 5.8	118, 218	5.93, 6.02
[22]	Rogers RO3003	41 × 44 × 1.52	2.4, 5.8	89, 301.6	3.74, 5.13
Proposed antenna	Felt	70 × 70 × 2.1	2.5, 3.6, 5.5	200, 285, 290	2.2, 0.3, 4.4

The reported work has advantages in terms of compactness, user comfort, multiband operation, and higher bandwidth with respect to other reported antennas.

5. CONCLUSION

In this paper, a compact dual-mode triple-band all textile antenna is proposed for wearable applications. The antenna is lightweight, compact in size and has a simple design topology in addition low backward radiation characteristics. The fundamental modes of both annular ring and triangular patch individually are responsible for the generation of broadside radiation pattern while the higher order modes of both result into monopole like radiation pattern. Simulated results are found in good agreement with the measured one.

REFERENCES

- [1] Song, C. T. P., P. S. Hall, H. Ghafouri-Shiraz, and D. Wake, "Triple band planar inverted F antennas for handheld devices," *Electronics Letters*, Vol. 36, No. 2, 112–114, 2000.
- [2] Mok, W. C., S. H. Wong, K. M. Luk, and K. F. Lee, "Single-layer single-patch dual-band and triple-band patch antennas," *IEEE Transactions on Antennas and Propagation*, Vol. 61, No. 8, 4341–4344, 2013.
- [3] Lee, K.-F., S. L. S. Yang, and A. A. Kishk, "Dual-and multiband U-slot patch antennas," *IEEE Antennas and Wireless Propagation Letters*, Vol. 7, 645–647, 2008.
- [4] Lee, K. F., K. M. Luk, K. M. Mak, and S. L. S. Yang, "On the use of U-slots in the design of dual-and triple-band patch antennas," *IEEE Antennas and Propagation Magazine*, Vol. 53, No. 3, 60–74, 2011.

- [5] Hsiao, F.-R. and K.-L. Wong, "Compact planar inverted-F patch antenna for triple-frequency operation," *Microwave and Optical Technology Letters*, Vol. 33, No. 6, 459–462, 2002.
- [6] Zhou, Y., C.-C. Chen, and J. L. Volakis, "Dual band proximity-fed stacked patch antenna for tri-band GPS applications," *IEEE Transactions on Antennas and Propagation*, Vol. 55, No. 1, 220–223, 2007.
- [7] Dang, L., Z. Y. Lei, Y. J. Xie, G. L. Ning, and J. Fan, "A compact microstrip slot triple-band antenna for WLAN/WiMAX applications," *IEEE Antennas and Wireless Propagation Letters*, Vol. 9, 1178–1181, 2010.
- [8] Mandal, B. and S. K. Parui, "Wearable tri-band SIW based antenna on leather substrate," *Electronics Letters*, Vol. 51, No. 20, 1563–1564, 2015.
- [9] Simorangkir, R. B. V. B., Y. Yang, L. Matekovits, and K. P. Esselle, "Dual-band dual-mode textile antenna on PDMS substrate for body-centric communications," *IEEE Antennas and Wireless Propagation Letters*, Vol. 16, 677–680, Aug. 2016.
- [10] Hong, Y., J. Tak, and J. Choi, "Dual-band dual-mode patch antenna for on–on–off WBAN applications," *Electronics Letters*, Vol. 50, No. 25, 1895–1896, 2014.
- [11] Wang, D., P. Li, and W.-S. Peng, "A novel design for a dual-mode triple-band communication terminal antenna based on the quadrifilar helix antenna and the BeiDou satellite navigation system," *Optik*, Vol. 127, No. 18, 7300–7311, 2016.
- [12] Wang, B. and Y. Lo, "Microstrip antennas for dual-frequency operation," *IEEE Transactions on Antennas and Propagation*, Vol. 32, No. 9, 938–943, 1984.
- [13] Zhang, X. and L. Zhu, "Patch antennas with loading of a pair of shorting pins toward flexible impedance matching and low cross polarization," *IEEE Transactions on Antennas and Propagation*, Vol. 64, No. 4, 1226–1233, 2016.
- [14] Jalil, M. E., M. K. A. Rahim, N. A. Samsuri, and N. A. Murad, "Triple band fractal koch antenna for wearable application," in *Progress In Electromagnetics Research Symposium Proceedings*, 1285–1289, KL, MALAYSIA, 2012.
- [15] Nagarjun, R., G. George, D. Thiripurasundari, R. Poonkuzhali, and Z. C. Alex, "Design of a triple band planar bow-tie antenna for wearable applications," in *2013 IEEE Conference on Information & Communication Technologies*, 1185–1189, IEEE, 2013.
- [16] Andreuccetti, D., "An Internet resource for the calculation of the dielectric properties of body tissues in the frequency range 10 Hz–100 GHz," <http://niremf.ifac.cnr.it/tissprop/>, 2012.
- [17] IEEE Standard C95.1-2005, "IEEE standard for safety levels with respect to human exposure to radio frequency electromagnetic fields, 3 kHz to 300 GHz," 2006.
- [18] Shirvani, P., F. Khajeh-Khalili, and M. H. Neshati, "Design investigation of a dual-band wearable antenna for tele-monitoring applications," *AEU — International Journal of Electronics and Communications*, Vol. 138, 153840, 2021.
- [19] Musa, U., S. M. Shah, H. B. A. Majid, M. K. A. Rahim, M. S. Yahya, Z. Yunusa, A. Salisu, and Z. Z. Abidin, "Wearable dual-band frequency reconfigurable patch antenna for WBAN applications," *Progress In Electromagnetics Research M*, Vol. 120, 95–111, 2023.
- [20] Le, T. T. and T.-Y. Yun, "Wearable dual-band high-gain low-SAR antenna for off-body communication," *IEEE Antennas and Wireless Propagation Letters*, Vol. 20, No. 7, 1175–1179, 2021.
- [21] Zhou, L., S. Fang, and X. Jia, "Dual-band and dual-polarised circular patch textile antenna for on-/off-body WBAN applications," *IET Microwaves, Antennas & Propagation*, Vol. 14, No. 7, 643–648, 2020.
- [22] Musa, U., S. M. Shah, H. A. Majid, I. A. Mahadi, M. K. A. Rahim, M. S. Yahya, and Z. Z. Abidin, "Design and analysis of a compact dual-band wearable antenna for WBAN applications," *IEEE Access*, Vol. 11, 30 996–31 009, 2023.